



Published in final edited form as:

*Acc Chem Res.* 2009 February 17; 42(2): 270–280. doi:10.1021/ar800127e.

## Characterization of Reactive Intermediates by Multinuclear Diffusion-Ordered NMR Spectroscopy (DOSY)

Deyu Li, Ivan Keresztes, Russell Hopson, and Paul G. Williard\*

*Department of Chemistry, Brown University, Providence, Rhode Island 02912*

### CONSPECTUS

Nuclear magnetic resonance (NMR) is the most powerful and widely utilized technique for determining molecular structure. Although traditional NMR data analysis involves the correlation of chemical shift, coupling constant, and NOE interactions to specific structural features, a largely overlooked method introduced more than 40 years ago, pulsed gradient spin-echo (PGSE), measures diffusion coefficients of molecules in solution, thus providing their relative particle sizes. In the early 1990s, the PGSE sequence was incorporated into a two-dimensional experiment, dubbed diffusion-ordered NMR spectroscopy (DOSY), in which one dimension represents chemical shift data while the second dimension resolves species by their diffusion properties. This combination provides a powerful tool for identifying individual species in a multicomponent solution—earning the nickname “chromatography by NMR.” In this Account, we describe our efforts to utilize DOSY techniques to characterize organometallic reactive intermediates in solution in order to correlate structural data to solid-state crystal structures determined by X-ray diffraction and to discover the role of aggregate formation and solvation states in reaction mechanisms.

In 2000, we reported our initial efforts to employ DOSY techniques in the characterization of reactive intermediates such as organolithium aggregates. Since then, we have explored DOSY experiments with various nuclei beyond  $^1\text{H}$ , including  $^6\text{Li}$ ,  $^7\text{Li}$ ,  $^{11}\text{B}$ ,  $^{13}\text{C}$ , and  $^{29}\text{Si}$ . Additionally, we proposed a diffusion coefficient-formula weight relationship to determine formula weight, aggregation number, and solvation state of reactive intermediates. We also introduced an internal reference system to correlate the diffusion properties of unknown reactive intermediates with known inert molecular standards, such as aromatic compounds, terminal olefins, cycloolefins, and tetraalkylsilanes. Furthermore, we utilized DOSY to interpret the role of aggregation number and solvation state of organometallic intermediates in the reactivity, kinetics, and mechanism of organic reactions. By utilizing multinuclear DOSY methodologies at various temperatures, we also correlated solid-state X-ray structures with those in solution and discovered new reactive complexes, including a monomeric boron enolate, a product-inhibition aggregate, and a series of intermediates in the vinyl lithiation of allyl amines. As highlighted by our efforts, DOSY techniques provide practical and feasible NMR procedures and hold the promise of even more powerful insights when extended to three-dimensional experiments.

\*To whom correspondence should be addressed. E-mail address: pgw@brown.edu..

## Introduction

Pulsed gradient spin-echo (PGSE) diffusion NMR spectroscopy was conceived to measure diffusion coefficients and deduce the hydrodynamic radii of molecules in solution in the mid-1960's by Stejskal & Tanner.<sup>1</sup> This occurred well before the necessary modern, sophisticated NMR instrumentation became routinely available to take advantage of the technique. In 1992, C.S. Johnson included the PGSE sequence into a two dimensional NMR experiment in which one dimension represents the regular chemical shift information and the second dimension separates species by particle size.<sup>2</sup> This 2D experiment is now referred to as diffusion-ordered NMR spectroscopy (DOSY). After discovering the benefits of DOSY, it is easy to appreciate why one polymer chemist has called this technique "chromatography by NMR" since NMR spectra of individual components of a complex mixture are easily resolved based upon their diffusion properties.<sup>3</sup> Recent excellent review articles surveyed the current state of the art from the perspective of an NMR specialist.<sup>4</sup>

In 2000, our group began to use DOSY to test the possibility of differentiating reactive intermediates such as dimeric and tetrameric *n*-BuLi aggregates based on their mobility.<sup>5</sup> Since then, we have published seven papers and eight presentations concerning reactive intermediates in which we rely heavily, if not exclusively, upon the DOSY technique to: (a) deconvolute the individual <sup>1</sup>H NMR spectra of organolithium aggregates in dynamic equilibrium with each other in solution; (b) demonstrate the two dimensional DOSY technique with variety of nuclei besides <sup>1</sup>H including <sup>6</sup>Li, <sup>7</sup>Li, <sup>11</sup>B, <sup>13</sup>C, and <sup>29</sup>Si; (c) correlate solution structures of aggregated and solvated organometallic compounds with solid state crystal structures; (d) determine aggregation number of dissolved organometallic intermediates; (e) determine the solvation state of organolithium aggregates in solution; (f) identify new organometallic aggregates in solution; (g) develop a set of internal references for our DOSY experiments that allow us to define a linear correlation to obtain molecular weights by NMR; (h) extract 1D NMR slices from DOSY spectra, which provide chemical shift information of every component in solution; (i) separate the individual NMR spectra of stereoisomers, such as a commercial mixture *cis*- & *trans*-cycloolefins (cyclododecenes) in solution, thereby pushing the limits of the concept of chromatography by NMR.

In our lab, DOSY techniques have been utilized to correlate solid state crystal structures determined by X-ray diffraction with solution structures and also to discover new aggregates participating in reaction mechanisms. Examples of these organometallic intermediates are depicted in Scheme 1 as follows: the tetramer (**1**) and dimer (**2**) of *n*-BuLi-THF complex,<sup>5</sup> the solvation and aggregation of vinylic lithiation intermediates (**3**),<sup>6</sup> aggregates containing lithium pinacolone enolate (**4**),<sup>7</sup> a monomeric boron enolate (**5**),<sup>8,9</sup> THF solvated LDA dimeric complex (**6**),<sup>10,11</sup> a mixed trimer (**7**) including *n*-BuLi and a chiral lithium amide, <sup>12,13</sup> a chiral lithium enolate trimer (**8**),<sup>14</sup> a complex consisting of lithium alkoxide and chiral lithium amide (**9**),<sup>15,16,17</sup> and alkali hexamethyldisilazide aggregates.<sup>18,19</sup>

Hence, we would like to present an account of progress and development of DOSY experiments in our lab focusing upon the characterization of highly reactive, transient organometallic intermediates from the point of view of a preparative chemist. This manuscript is organized into two sections: the first part outlines multinuclear DOSY methods and diffusion coefficient-formula weight correlations; the second part focuses on the application of these methods in characterizing reactive organometallic intermediates in solution.

## Part I. Multinuclear DOSY Techniques

### $^1\text{H}$ DOSY and 2D Separations

$^1\text{H}$ -detected DOSY is the major diffusion NMR technique among all NMR sensitive nuclei. It has emerged as a promising technique in polymer physics, combinatorial chemistry and enzymatic dynamic studies.<sup>4</sup> We carry out  $^1\text{H}$  DOSY extensively due to the sensitivity and convenience of  $^1\text{H}$  NMR.

To establish the usefulness of the DOSY technique in identification of organometallic intermediates, our initial studies focused on *n*-BuLi in THF solution since *n*-BuLi is easily accessible and its solution structure is well characterized. *n*-BuLi was shown to exist in equilibrium between tetrasolvated dimeric and tetrasolvated tetrameric aggregates in THF solutions by NMR spectroscopy and cryoscopy.<sup>6</sup> The solid-state structures of the tetrameric aggregate and a TMEDA solvated dimer have also been determined by X-ray crystallography.<sup>6</sup>

Our diffusion-ordered NMR experiments were initially performed with  $^1\text{H}$  and  $^7\text{Li}$  detection.  $^1\text{H}$  DOSY experimental datasets were processed and presented in a 2D DOSY form<sup>2</sup> (Figure 1). In the  $^1\text{H}$  DOSY spectrum; the resolved  $\alpha$  and partially resolved  $\beta$  and  $\gamma$   $\text{CH}_2$  groups in the dimer are centered at a higher diffusion coefficient value than the corresponding peaks in the tetrameric aggregate. The NMR spectra of the individual dimer and tetramer aggregates are very well separated from the solutes hexanes and THF. Relative diffusion coefficients were determined by fitting the peak areas to the Stejskal-Tanner equation<sup>20</sup> (Figure 2). Diffusion coefficients determined from  $^7\text{Li}$ -detected experiments were in good agreement with  $^1\text{H}$  DOSY results.<sup>5</sup> This was our first successful application of DOSY to distinguish relatively small reactive organolithium aggregates in solution.

Currently, we can routinely characterize a solution consisting of several components with different sizes by a single DOSY experiment. An example is shown in Figure 3. The  $^1\text{H}$  DOSY spectrum of an amino ether ligand **10**, 1-octadecene (ODE), cyclododecene (CDDE), and benzene in toluene- $d_8$  solution separates into four components in the diffusion dimension. In increasing order of diffusion coefficient (decreasing formula weight) these are the ligand **10** ( $\text{C}_{17}\text{H}_{39}\text{NOSi}$ , mw 301.6), ODE ( $\text{C}_{18}\text{H}_{36}$ , mw 252.3), CDDE ( $\text{C}_{12}\text{H}_{22}$ , mw 166.3) and benzene ( $\text{C}_6\text{H}_6$ , mw 78.1). The  $^1\text{H}$  signals of the protons 1, 1', 2, 3 and 5 in ligand **10** have identical diffusion coefficients. The  $^1\text{H}$  chemical shifts of ODE, CDDE, and benzene are also well separated in the diffusion dimension.

### $^{13}\text{C}$ INEPT DOSY Technique

Reports of  $^1\text{H}$ -DOSY experiments continue to increase,<sup>4</sup> however, very few  $^{13}\text{C}$  INEPT DOSY spectra have been reported although they provide better resolution, a wider chemical shift range than proton spectra and absence of homonuclear coupling.<sup>4e</sup>

To establish the effectiveness of the  $^{13}\text{C}$  INEPT DOSY technique, we performed initial studies utilizing commercially available THF-solvated lithium diisopropylamide (LDA) dimer **6**,<sup>10</sup> the most prominent non-nucleophilic base used in organic synthesis and also an ideal candidate for investigating organolithium aggregation states.<sup>21</sup> It exists as a single major form—THF disolvated dimer—in THF solution<sup>21</sup> as depicted in Figure 4. In this study we choose ODE, CDDE and benzene as the internal references due to their chemical inertness and suitable NMR properties. A detailed discussion of internal reference system will be presented in the following section.

The  $^{13}\text{C}$  INEPT DOSY spectrum of THF solvated LDA dimer **6** with the three internal references indicated above in toluene- $d_8$  solution resolves all six components in the diffusion

dimension. These are clearly identifiable in the DOSY spectrum as labeled in Figure 4. In increasing order of diffusion coefficient (decreasing radii) these are the LDA-THF dimer ( $C_{20}H_{44}Li_2N_2O_2$ , mw 351.5), ODE ( $C_{18}H_{36}$ , mw 252.3), *cis*-CDDE ( $C_{12}H_{22}$ , mw 166.3), *trans*-CDDE ( $C_{12}H_{22}$ , mw 166.3), ethylbenzene ( $C_8H_{10}$ , mw 106.2) and benzene ( $C_6H_6$ , mw 78.1). It is noteworthy that the diffusion dimension separation of *cis*- and *trans*-CDDE is seen as they have exactly the same formula weight and are observed to exhibit only a 3.17% difference in relative diffusion coefficient. The  $^{13}C$  INEPT signals of the oxygen-attached carbons in THF ( $\delta = 68.5$  ppm) and the LDA methine carbons ( $\delta = 51.8$  ppm) have identical diffusion coefficients. This evidence corroborates the integrity of THF and LDA aggregate in solution and suggests that THF and LDA remain attached and detectable under the experimental conditions.

### Diffusion Coefficient and Formula Weight Correlation

Diffusion coefficients and molecular radii are correlated theoretically by the Stokes-Einstein equation<sup>4e</sup> (Equation 1:  $D = kT/6\pi\eta r$ ).<sup>22</sup> Comparison of numerous solid state X-ray crystal structures carried out in our lab reveals that the densities of all organolithium aggregates are very similar, i.e.  $\sim 1.0$  g/cm<sup>3</sup>. Also we note that all the aggregates we have observed are relatively spherical.<sup>23</sup> Hence we can postulate that the volume of an aggregate is proportional to its formula weight. Thus there should be a linear correlation between the diffusion coefficient determined by DOSY and FW (Equation 2:  $D \sim FW^a$ ).<sup>24</sup> The equation is linearized by taking the logarithm of both sides (Equation 3:  $\log D = a \log FW + b$ ).

According to Equation 3, there will be a linear correlation between measured diffusion coefficients and the formula weights of aggregates in solution. Hence, we were able to use the FW of known molecules in order to establish a calibration curve. Empirical FWs of unknown aggregates are interpolated from the curve thereby providing us with a rapid and convenient determination of these values.

To test this method, we applied it to a THF solution containing a mixture of LDA, lithium pinacolonate **4** (LPN), and diaisopropylamine **12** (DIPA). LDA is known to form exclusively a disolvated cyclic dimer **6**, while LPN exists as an equilibrium mixture of a tetrasolvated dimer **14** and tetrasolvated cubic tetramer **15**. In addition to these aggregates, LDA and LPN were shown to form a mixed trisolvated dimer **13** containing one lithium amide and one enolate residue (Scheme 2).

DSTE-LED DOSY experiments were performed and decay curves were determined from peak intensities of all peaks. The decay curves were linearized (Figure 5), but the absolute diffusion coefficients were not calculated. Instead, the slopes of the decay curves were plotted as a function of FW, as defined in Equation 2 (Figure 6, left) and Equation 3 (Figure 6, right). Reasonably linear correlations were obtained for both plots. The positive results appeared to validate the method discussed above and indicate that the FW of unknown aggregates can be determined in this fashion. These results indicate that inclusion of solvent, known aggregates or intentionally added molecules as internal FW references provides a promising method to deduce the aggregation number and solvation state of an unknown complex.

### Internal References System

DOSY spectra often include artifacts generated by temperature fluctuation, convection, and viscosity change.<sup>25</sup> Hence the internal reference method<sup>26</sup> strives to eliminate the complications of these effects while taking advantage of the benefits of DOSY spectra. Consequently, one can determine aggregation numbers and solvation states accordingly. This methodology extends and simplifies the current NMR techniques such as analysis of quadrupole coupling, multiplicity and bimolecular exchange, HMPA titration and Job plots

that have been employed for determining aggregation states of reactive intermediates in solution.<sup>10</sup>

Due to their chemical and NMR properties, there are several requirements for internal references: (a) they should be inert to the components in solution; (b) the chemical shifts of these internal references should not overlap with other components; (c) the internal references should have no or little coordinating ability to the complexes in solution; (d) they should have good solubility in the NMR solvents; (e) they should possess desirable molecular weight distributions.

We chose four types of molecule (Scheme 3) as internal references: Type one: aromatic compounds, like benzene **16** and perylene **17**; type two: cycloolefins, such as *cis*-CDDE **18** and *trans*-CDDE **19** and COE **20**; type three: terminal olefins, such as ODE **21** and TDE **22**; type four: tetraalkyl silane, such as TMS **23**. We utilize three internal reference combinations, such as ODE/CDDE/benzene or TDE/COE/benzene in the DOSY investigations.

For example, the <sup>13</sup>C INEPT DOSY results (Figure 4) of LDA-THF dimer **6** strongly suggest that the diffusion coefficients and formula weights of LDA-THF dimer **6**, ethylbenzene and the three internal references, ODE, CDDE and benzene, can be utilized to define a linear correlation between the relative log *D* and log FW. The correlation between log FW and log *D* of the linear least squares fit to reference points of all components in this mixture is extremely high,  $r^2 = 0.9971$ . This remarkable result highlights the ability to use suitable internal references in DOSY experiments to interpolate relative diffusion coefficients and formula weights, and by inference, solvation and aggregation states of the bis-THF solvated LDA dimer **6**.

### DOSY Extracted 1D Spectrum Slices

An added bonus of 2D DOSY spectra is to extract a one dimensional spectrum slice at the diffusion coefficient of a particular species. The extracted spectrum provides the chemical shift information of the corresponding species.

DOSY spectrum of ligand **10** in Figure 3 shows a good separation of four components in the diffusion dimension. Their DOSY 1D <sup>1</sup>H slice shows the complete chemical shift resolution among all components. To emphasize this point, we have depicted peaks of ligand **10** ( $\delta = 3.66, 3.60, 2.84, 2.35$  and  $1.85$  ppm) in the slice of ligand **10** (Figure 7b) to be compared with the spectrum of the pure, authentic sample (Figure 7b'). <sup>1</sup>H NMR slices taken at the diffusion coefficients of ligand **10** and the internal references agree very well with their respective <sup>1</sup>H NMR spectra. Hence, the <sup>1</sup>H spectra extracted from the single 2D <sup>1</sup>H DOSY experiment resolved chemical shift information of every component in the mixture.

Because <sup>13</sup>C INEPT DOSY provides a better resolution than <sup>1</sup>H DOSY in the chemical shift dimension, its 1D DOSY slice is a mimic of regular <sup>13</sup>C INEPT NMR spectrum and it also permits an unambiguous assignment of <sup>13</sup>C signals for every component in a mixture. <sup>13</sup>C INEPT DOSY of LDA-THF dimeric aggregate **6** is an ideal example to highlight this point. We depict peaks of LDA ( $\delta = 68.5$  ppm) and THF ( $\delta = 51.8$  ppm) in the slice of LDA-THF aggregate (Figure 8b) to be compared with the spectrum of the pure, authentic sample (Figure 8b'). Slices taken at other diffusion coefficients of the components agree extremely well with their respective <sup>13</sup>C INEPT spectra. Hence, the extracted INEPT spectra determined from the single 2D INEPT DOSY experiment completely resolved chemical shift information of every component in the mixture.

The DOSY slices in Figure 9 also illustrate the complete chemical shift resolution of nearly identical signals of benzene ( $\delta = 128.38$  ppm) and ethylbenzene ( $\delta = 128.41$  ppm). We also call attention to the fact that although the difference of relative diffusion coefficient between



*cis*- and *trans*-CDDE is observed to be only 3.17%, spectra slices of the pure *trans*- and nearly pure *cis*-CDDE isomers can be resolved as depicted in Figure 10.

## Part II. Identification of Reactive Intermediates

### Confirmation of Solid-State Structures

While X-ray crystallographic methods are most widely used for solid-state structure determination, questions remain concerning the relationship between solution state structures of reactive intermediates and those in solid state. A relevant question concerning the structural integrity of an organometallic complex in these two very different phases is whether the structure determined in the solid state represents the only, the major, or one among several species in the solution. One must also address whether, and how easily any stereostructure changes occur in solution relative to solid state. Therefore, solution structure determination represents a critical complement to X-ray structure determination of organometallic aggregates. We utilize a new NMR strategy combining multinuclear DOSY and other 1D/2D NMR techniques to characterize organometallic complexes in solution.

#### Example 1: Monomeric Boron Enolate of *tert*-Butyl Methyl Ketone (5)

A boron enolate **5** was investigated by X-ray crystallography and a  $^1\text{H}$  DOSY experiment (Figure 11).<sup>8</sup> On the basis of diffusion coefficients from DOSY, the relative ratio of the hydrodynamic radii of enolate **5** and the internal reference perylene **17** is 1.186. For comparison, the geometry of these compounds was optimized by DFT calculations, and the theoretical ratio of the hydrodynamic radii was determined to be 1.155, which agrees well with the experimentally derived value. The DOSY results unambiguously indicate that enolate **5** exists exclusively as a monomer in benzene solution.

### Discovery of New Reactive Intermediates

As implied by the name “reactive intermediate”, it is often difficult to isolate and identify such species by conventional means such as X-ray diffraction. NMR and other spectroscopic techniques are better suited for characterizing sensitive intermediates in reaction pathways. DOSY methods provide a unique perspective for observing the size, shape, and formula weight of these intermediates. This information is valuable for understanding the aggregation number and solvation state of those transitional complexes. The use of DOSY and other NMR techniques have enabled us to identify several reactive aggregates that play important roles in reaction pathways.

#### Example 2: Intermediates of Vinylic Lithiation of Allylamine Derivatives

Treatment of allyl alcohol and allylamine derivatives with strong base effects reactions in which synthetically useful allylanions are formed.<sup>6</sup> An alternative to allylic deprotonation is observed with secondary allylamines. These compounds can undergo vinylic deprotonation at the 3-position (Scheme 4). This reaction is observed exclusively upon reaction of *N*-monoalkyl and *N*-silyl allylamine with alkyl lithium reagents. NMR work strongly indicated that the dianion derived from allylamine **24**, 3, *N*-dilithio-*N*-(*tert*-butyldimethylsilyl)allylamine (**3**), retains the “c-clamp” like structure observed in the solid state (Scheme 4).<sup>27</sup> A total of five aggregates of **3** could be assigned, three homoaggregates **26–28**, an *n*-BuLi containing mixed aggregate **29** and a mixed aggregate **30** containing one molecule each of **3**, *n*-BuLi and *n*-BuOLi (Scheme 5). Information about aggregation numbers was obtained from  $^1\text{H}$  DOSY experiments.

Our approach for solutions containing mixtures of aggregates is to estimate the formula weight (FW) of each aggregate by correlating their experimentally determined mobility and expected MW. Success of this method requires additional information upon the structure of at least some

of the known aggregates so that educated guesses can be made regarding possible MW values. We use the solvent and aggregates of known composition as internal reference, whenever possible. In this case, we used the FW of the *n*-BuLi dimer **1** (Scheme 1) in conjunction with residual THF-*d*<sub>7</sub> as our starting point for correlating experimental mobilities and MW's. The MW's were then adjusted by varying the number of lithium amide residues in the homoaggregates and the composition and number of coordinated THF ligands in all aggregates, until the best possible correlation was obtained (Figure 12, Table 1). All proposed structures were confirmed to be minima on the potential energy surface by PM3 semi-empirical calculations.<sup>6</sup> The best fit for the higher order aggregate **28** actually corresponded to a THF monosolvated trimer. That structure was rejected because <sup>1</sup>H NMR spectrum of this complex has only a single set of resonances of intermediate **3** and is absent of THF signal. Deviation from the calibration curve is attributed to the cylindrical shape of the tetrameric aggregate.

### Example 3: Chiral Lithium Alkoxide Complex (9)

<sup>1</sup>H and <sup>13</sup>C INEPT DOSY were utilized to characterize a new trimeric complex **9** (Scheme 1) between two equiv lithium amide and one equiv lithium alkoxide. Observation of this new mixed aggregate strongly indicates the possibility of product-induced chirality inhibition that is detrimental to the enantioselectivity of asymmetric addition reaction (Scheme 6). This conclusion was based upon the reaction pathways in Scheme 7 in which the formation of complex **9** destroys the integrity of the chiral aggregate **7**, which is responsible for the asymmetric butylation of aldehydes.

We chose ODE **21** as the internal reference for our DOSY experiments. The <sup>1</sup>H DOSY spectrum of mixed trimeric complex **9** with ODE in toluene-*d*<sub>8</sub> solution separates into two components in the diffusion dimension. These are clearly identifiable in the DOSY spectrum reproduced in Figure 13. In increasing order of diffusion coefficient (decreasing formula weight) these are the complex **9** (C<sub>43</sub>H<sub>95</sub>Li<sub>3</sub>N<sub>2</sub>O<sub>3</sub>Si<sub>2</sub>, FW 765.2) and ODE (C<sub>18</sub>H<sub>36</sub>, mw 252.3). The <sup>1</sup>H signals of the protons 1, 1', 2, 3 and 5 on ligand and proton 9 on alkoxide in complex **9** (Figure 13) have identical diffusion coefficients. The similar diffusion behavior confirms that the lithium alkoxide and the lithium amide are in the same complex. As we have previously noted, <sup>1</sup>H DOSY results allow us to correlate the diffusion coefficients and formula weights of complex **9**, ODE and toluene-*d*<sub>8</sub>. The correlation between log FW and log *D* of the linear least squares fit to reference points of all components in this mixture is extremely high, *r*<sup>2</sup> = 0.9961.<sup>15</sup> This result unambiguously establishes complex **9** as a mixed trimeric aggregate consisting of 2 equiv lithium amide and 1 equiv lithium alkoxide. The <sup>13</sup>C INEPT DOSY results show similar results (Figure 14).

### Limitations and Future Directions

<sup>1</sup>H DOSY analysis is often hindered by the small chemical shift scale and homonuclear coupling resulting in a spectrum with overlapping signals whose diffusion coefficient can not be accurately extracted. Efforts to overcome signal overlap include use of <sup>1</sup>H-homodecoupled or 'pure shift' DOSY experiments<sup>28</sup> or performing heteronuclear DOSY on a nucleus, such as <sup>13</sup>C, with a wider chemical shift scale.<sup>4e</sup>

Heteronuclear-detected DOSY, such as <sup>13</sup>C DOSY, provides better resolution than proton spectra due to its wider chemical shift range. <sup>19</sup>F diffusion NMR analysis<sup>29</sup> and <sup>31</sup>P-detected DOSY<sup>30</sup> employ pulse sequences similar to <sup>1</sup>H DOSY because their nuclei have high-natural abundance and gyromagnetic ratio. <sup>13</sup>C INEPT-DOSY and <sup>29</sup>Si DOSY<sup>31</sup> pulse sequences have been developed for studying multi-species solutions. However, no <sup>6</sup>Li-detected and very few <sup>7</sup>Li DOSY<sup>4d</sup> investigations of organolithium were published prior to our studies.

Another promising area of DOSY analysis is the three-dimensional DOSY method. For nuclei of low natural abundance, coherence transfer from proton to heteronuclear atoms and then back to proton for detection can significantly improve their sensitivity. In 3D DOSY<sup>4e-4g</sup> experiments, a coordinate of diffusion is added to the conventional 2D NMR experiments. The aim of these techniques is to obtain additional dispersion of NMR peaks on a third axis on the basis of their diffusion coefficients. These experiments can reduce overlapping NMR signals in the traditional 1D and 2D NMR thus making them particularly useful for identifying various species in a multi-components solution. The first 3D DOSY experiment reported was a NOESY-DOSY sequence,<sup>32</sup> in which the overlapping peaks of a DNA duplex and a dinucleotide were separated. Since then, other 3D DOSY sequences, such as DOSY-TOCSY,<sup>33</sup> DOSY-HMQC,<sup>31,34</sup> COSY-IDOSY<sup>35</sup> and 2DJ-IDOSY,<sup>36</sup> have been developed. We plan to extend DOSY studies in our lab<sup>37</sup> to additional heteronuclear and 3D detections and to combine them into 3D heteronuclear DOSY techniques.

## Conclusions

In the above sections, we presented our results on the characterization of reactive intermediates, especially the aggregation number and solvation state of the complexes. To obtain useful information of the aggregates, we rely greatly on the multinuclear DOSY NMR techniques, especially the <sup>1</sup>H and <sup>13</sup>C DOSY methods. In the first part we proved an effective DOSY-related NMR strategy for identifying individual species in a multi-component mixture solution. This strategy includes the particle size-dependent separation on the diffusion dimension in the DOSY spectrum, diffusion coefficient and formula weight correlation, an efficient internal reference system, and the 1D spectrum slice from 2D DOSY spectra. In the second part, we applied the above strategy at various temperatures to investigate the solution state structure of a range of organometallic intermediates. Multinuclear DOSY techniques were not only used to confirm solid state X-ray crystal structures but also to discover new complexes that confer significant effect on the reactivity, kinetics and mechanism of organic reactions. We also discussed the limitations of the traditional DOSY methods and the feasible solution for these problems: heteronuclear and 3D DOSY techniques. These DOSY methods and applications should be beneficial for chemists to explore other reactive intermediates in solution.

## Acknowledgment

Our work has been supported through the National Science Foundation Grant 0718275 and the National Institutes of Health Grant GM-35982. We thank former and current PGW group members for their contributions, especially Dr. Madeleine A. Jacobson, Dr. Jia Liu, Dr. Lili Ma, Mr. Weibin Li, and Mr. Gerald L. Kagan.

## BIOGRAPHICAL INFORMATION

**Deyu Li** received his B.S. degree (1996) from Beijing Medical University and M.S. degree from Chinese Academy of Medical Sciences (1999). He is currently a graduate student in the Williard group at Brown University. His research experience includes synthetic methodology, NMR investigations of reaction mechanism, and natural product chemistry.

**Ivan Keresztes** received his B.A. from Bard College (1996) and Ph.D. from Brown University (2002). In 1997, he joined the Williard group and pursued research in developing new NMR methodologies for the solution state characterization of organolithium aggregates. He did post-doctoral work at the University of Pennsylvania with George Furst. He is currently the Director of the NMR facility in the Department of Chemistry and Chemical Biology of Cornell University.



**Russell Hopson** obtained his B.S. from George Mason University in 1994, and his Ph.D. from Northeastern University in 2000. He worked in industry for the Gillette Co. throughout his entire graduate career and for two years at the Clariant Corporation after receiving his doctorate. He has been the NMR facility supervisor in the Chemistry Department of Brown University for the last 4 years where he maintains the NMR spectrometers, conducts training, and routinely collaborates with faculty and students in various fields of research.

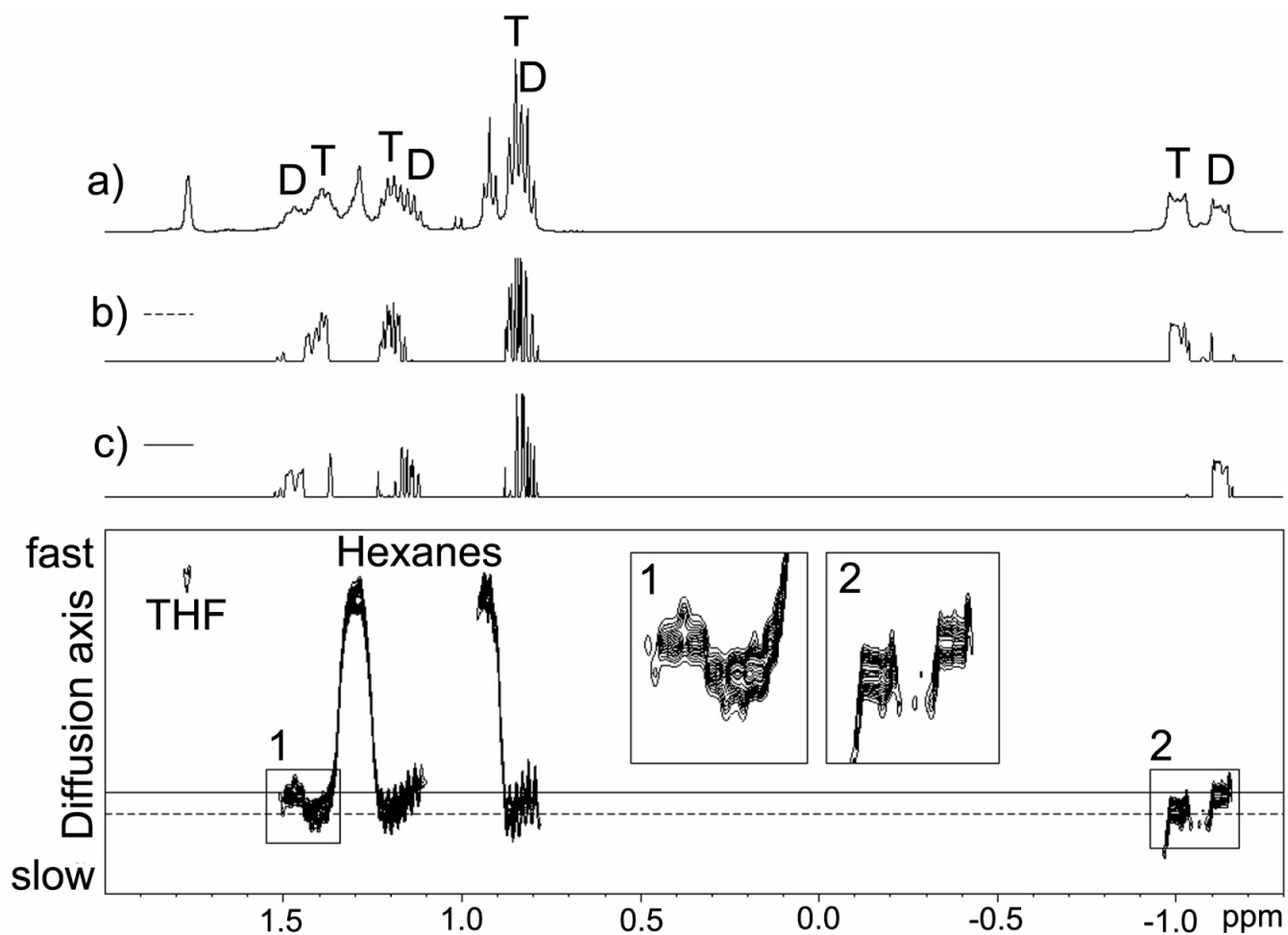
**Paul G. Williard** obtained a combined B.S./M.S. degree from Bucknell University in 1972 working with Harold W. Heine and a Ph.D. degree from Columbia University in 1976 under the supervision of Gilbert Stork where he developed a strong interest in enolates and enolate reactions. He pursued post-doctoral work with George Büchi at MIT and began his independent career at Brown University in 1979. He served as department chair from 1999–2005 and currently is a Professor of Chemistry at Brown. His research program focuses on discovery and characterization of reactive anionic intermediates in the solid state and in solution.

## REFERENCES

1. (a) Stejskal EO, Tanner JE. Spin diffusion measurements: spin echoes in the presence of a time-dependent field gradient. *J. Chem. Phys* 1965;42:288–292. (b) Tanner JE. Pulsed field gradients for N.M.R. spin-echo diffusion measurements. *Rev. Sci. Instrum* 1965;36:1086–1087. (c) Stejskal EO. Use of spin echoes in a pulsed magnetic-field gradient to study anisotropic, restricted diffusion and flow. *J. Chem. Phys* 1965;43:3597–3603.
2. Morris KF, Johnson CS Jr. Diffusion-ordered two-dimensional nuclear magnetic resonance spectroscopy. *J. Am. Chem. Soc* 1992;114:3139–3141.
3. Gounarides JS, Chen A, Shapiro MJ. Nuclear magnetic resonance chromatography: applications of pulse field gradient diffusion NMR to mixture analysis and ligand-receptor interactions. *J. of Chromatography, B: Biomed. Sci. Appl* 1999;725:79–90.
4. (a) Macchioni A, Ciancaleoni G, Zuccaccia C, Zuccaccia D. Determining accurate molecular sizes in solution through NMR diffusion spectroscopy. *Chem. Soc. Rev* 2008;37:479–489. [PubMed: 18224258] (b) Antalek B. Using PGSE NMR for chemical mixture analysis: Quantitative aspects. Concepts in Magnetic Resonance Part A 2007;30A:219–235. (c) Brand T, Cabrita EJ, Berger S. Theory and application of NMR diffusion studies. *Modern Magnetic Resonance* 2006;1:131–139. (d) Pregosin PS, Kumar PGA, Fernandez I. Pulsed gradient spin-echo (PGSE) diffusion and  $^1\text{H}$ ,  $^{19}\text{F}$  heteronuclear Overhauser spectroscopy (HOESY) NMR methods in inorganic and organometallic chemistry: something old and something new. *Chem. Rev* 2005;105:2977–2998. [PubMed: 16092825] (e) Cohen Y, Avram L, Frish L. Diffusion NMR spectroscopy in supramolecular and combinatorial chemistry: An old parameter - new insights. *Angew. Chem., Int. Ed* 2005;44:520–554. (f) Morris, Gareth A. Diffusion-ordered spectroscopy (DOSY). *Encyclopedia of Nuclear Magnetic Resonance* 2002;9:35–44. (g) Johnson CS Jr. Diffusion ordered nuclear magnetic resonance spectroscopy: principles and applications. *Prog. Nucl. Magn. Reson. Spectrosc* 1999;34:203–256. (h) Fernandez I, Martinez-Viviente E, Breher F, Pregosin PS.  $^7\text{Li}$ ,  $^{31}\text{P}$ , and  $^1\text{H}$  pulsed gradient spin-echo (PGSE) diffusion NMR spectroscopy and ion pairing: On the temperature dependence of the ion pairing in  $\text{Li}(\text{CPh}_3)$ , fluorenyllithium, and  $\text{Li}[\text{N}(\text{SiMe}_3)_2]$  amongst other salts. *Chem.- Eur. J* 2005;11:1495–1506.
5. Keresztes I, Williard PG. Diffusion-ordered NMR spectroscopy (DOSY) of THF solvated *n*-butyllithium aggregates. *J. Am. Chem. Soc* 2000;122:10228–10229.
6. Jacobson MA, Keresztes I, Williard PG. On the mechanism of THF catalyzed vinylic lithiation of allylamine derivatives: Structural studies using 2-D and diffusion-ordered NMR spectroscopy. *J. Am. Chem. Soc* 2005;127:4965–4975. [PubMed: 15796563]
7. Keresztes, I. Ph.D. Dissertation. Brown Univ.; 2002.
8. Ma L, Hopson R, Li D, Zhang Y, Williard PG. Synthesis and structural characterization of the bis (diisopropylamino)boron enolate of *tert*-Butyl methyl ketone. *Organometallics* 2007;26:5834–5839.
9. Ma, L.; Hopson, R.; Williard, PG. Structural studies of boron enolates by X-ray crystallography and DOSY NMR spectroscopy. Abstracts of Papers, 234th ACS National Meeting; Boston, MA, United States. August 19-23; 2007. ORGN-023

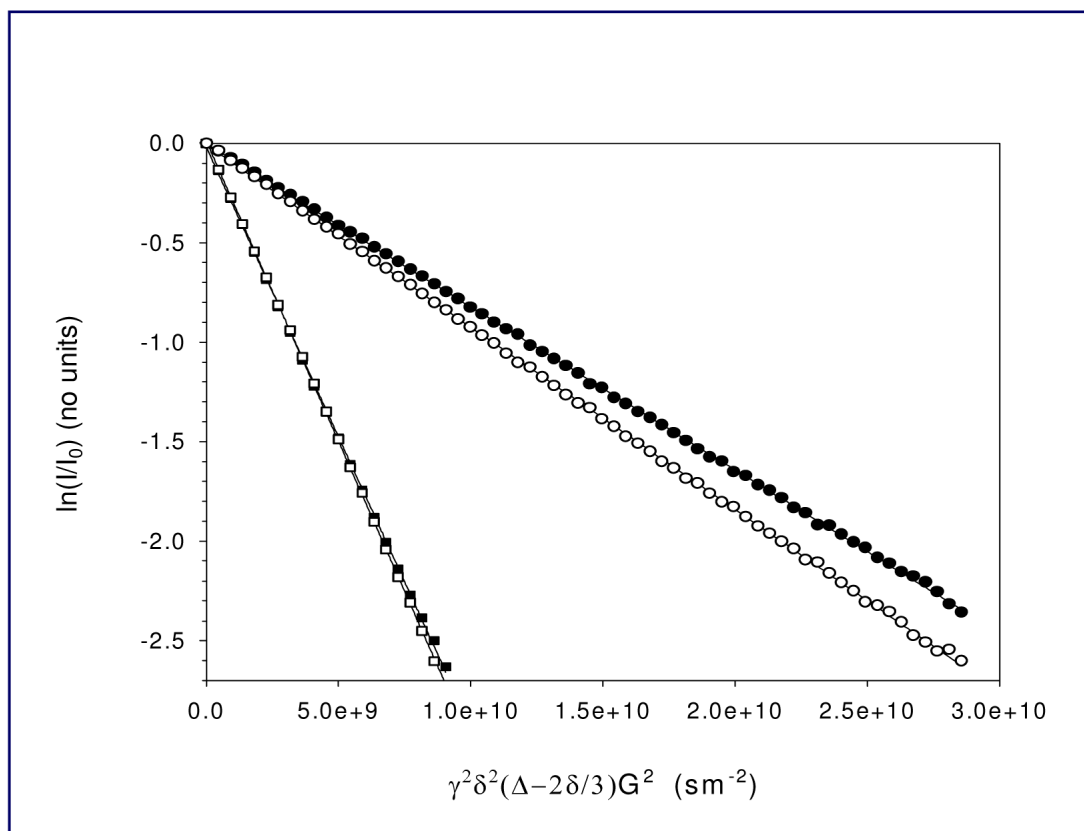
10. Li D, Hopson R, Li W, Liu J, Williard PG.  $^{13}\text{C}$  INEPT diffusion-ordered NMR spectroscopy (DOSY) with internal references. *Org. Lett* 2008;10:909–911. [PubMed: 18251549]
11. Li, D.; Liu, J.; Williard, PG.  $^{13}\text{C}$  DOSY studies of solution structures of lithium diisopropylamide and alkali hexamethyldisilazides. Abstracts of Papers, 233rd ACS National Meeting; Chicago, IL, United States. March 25-29; 2007. INOR-1018
12. Li D, Sun C, Liu J, Hopson R, Li W, Williard PG. Aggregation studies of complexes containing a chiral lithium amide and *n*-butyllithium. *J. Org. Chem* 2008;73:2373–2381. [PubMed: 18294002]
13. Liu, J.; Li, D.; Williard, PG. NMR studies on mixed trimer complex of *n*-BuLi and chiral lithium amide. Abstracts of Papers, 232nd ACS National Meeting; San Francisco, CA, United States. Sept. 10-14; 2006. ORGN-172
14. Li, D.; Li, W.; Williard, PG. Solution-state structures of chiral mixed aggregates by Diffusion-Ordered NMR spectroscopy. Abstracts of Papers, 235th ACS National Meeting; New Orleans, LA, United States. April 6-10; 2008. ORGN-097
15. Liu J, Li D, Sun C, Williard PG. Analysis of an asymmetric addition with a 2:1 mixed lithium amide / *n*-butyl lithium aggregate. *J. Org. Chem* 2008;73ASAP
16. Li, D.; Liu, J.; Williard, PG. Multinuclear DOSY studies of organometallic systems. Abstracts of Papers, 233rd ACS National Meeting; Chicago, IL, United States. March 25-29; 2007. ORGN-282
17. Li, D.; Li, W.; Williard, PG. Internal-standard system of multinuclear diffusion-ordered NMR spectroscopy and its applications in identification of organometallic complexes. Abstracts of Papers, 234th ACS National Meeting; Boston, MA, United States. August 19-23; 2007. ORGN-851
18. Li, D.; Liu, J.; Williard, PG. Diffusion-ordered NMR spectroscopy (DOSY) studies of mixed alkali metal cation hexamethyldisilazide bases. Abstracts of Papers, 232nd ACS National Meeting; San Francisco, CA, United States. Sept. 10-14; 2006. ORGN-166
19. Li, D.; Li, W.; Williard, PG. Lithium diisopropylamide and lithium hexamethyldisilazide aggregation state studies by diffusion-ordered NMR spectroscopy. Abstracts of Papers, 235th ACS National Meeting; New Orleans, LA, United States. April 6-10; 2008. INOR-736
20. (a) Jerschow A, Müller N. Suppression of convection artifacts in stimulated-echo diffusion experiments. Double-stimulated-echo experiments. *J. Magn. Reson* 1997;125:372–375. (b) Hilmersson G, Davidsson O. Stereogenic lithium centers in a complex between *n*-butyllithium and a dilithiated chiral amine - solution studies by Li-6, H-1-hoesy, Li-6,Li-6-cosy, and Li-6,Li-6-exsy nmr. *Organometallics* 1995;14:912–918.
21. Collum DB, McNeil AJ, Ramirez A. Lithium diisopropylamide: Solution kinetics and implications for organic synthesis. *Angew. Chem., Int. Ed* 2007;46:3002–3017.
22.  $D = (kT)/(6\pi\eta r)$ , where  $D$  is the diffusion coefficient,  $k$  is the Boltzman constant,  $T$  is the temperature in Kelvin,  $\eta$  is the viscosity of the solution, and  $r$  is the radius of the molecular sphere.
23. From different DOSY experiments, we proved our spherical assumption is good for small molecule systems.
24. For monodispersed polymer system, it has been found that  $D$  is related to molar mass  $M$  of the polymer by:  $D = AM^a$  ( $A = 10^{-7.62}$  and  $a = -0.62$ ). See: Chen A, Johnson CS. Determination of molecular-weight distributions for polymers by diffusion-ordered NMR. *J. Am. Chem. Soc* 1995;117:7965–7970. We can linearize this equation by taking the logarithm of both sides and get the equation below:  $\log D = a \log M + \log A$ . Or simplify it to:  $\log D = a \log FW + b$ , where  $b = \log A$  and  $FW$  is  $M$ .
25. Sorland GH, Aksnes D. Artefacts and pitfalls in diffusion measurements by NMR. *Magn. Reson. in Chem* 2002;40:S139–S146.
26. (a) Groves P, Rasmussen MO, Molero MD, Samain E, Canada FJ, Driguez H, Jimenez-Barbero J. Diffusion ordered spectroscopy as a complement to size exclusion chromatography in oligosaccharide analysis. *Glycobiology* 2004;14:451–456. [PubMed: 14693914] (b) Cabrita EJ, Berger S. DOSY studies of hydrogen bond association: tetramethylsilane as a reference compound for diffusion studies. *Magn. Reson. Chem* 2001;39:S142–148.
27. Williard PG, Jacobson MA. Dianion aggregates derived from lithiation of *N*-silyl allylamine. *Org. Lett* 2000;2:2753–2755. [PubMed: 10964357]
28. Nilsson M, Morris GA. Pure shift proton DOSY: diffusion-ordered H-1 spectra without multiplet structure. *Chem. Comm* 2007:933–935. [PubMed: 17311125]

29. Derrick TS, Lucas LH, Dimicoli JL, Larive CK. F-19 diffusion NMR analysis of enzyme-inhibitor binding. *Mag. Reson. Chem* 2002;40:S98–S105.
30. Kapur GS, Cabrita EJ, Berger S. The qualitative probing of hydrogen bond strength by diffusion-ordered NMR spectroscopy. *Tetrahedron Lett* 2000;41:7181–7185.
31. Stchedroff MJ, Kenwright AM, Morris GA, Nilsson M, Harris RK. 2D and 3D DOSY methods for studying mixtures of oligomeric dimethylsiloxanes. *Phys. Chem. Chem. Phys* 2004;6:3221–3227.
32. Gozansky EK, Gorenstein DG. DOSY-NOESY: Diffusion-ordered NOESY. *J. Magn. Reson* 1996;111:94–96. Series B
33. (a) Bradley SA, Krishnamurthy K, Hu H. Simplifying DOSY spectra with selective TOCSY edited preparation. *J. Magn. Reson* 2005;172:110–117. [PubMed: 15589414] (b) Jerschow A, Müller N. 3D diffusion-ordered TOCSY for slowly diffusing molecules. *J. Magn. Reson* 1996;123:222–225. Ser. A
34. Barjat H, Morris GA, Swanson GA. A three-dimensional DOSY-HMQC experiment for the high-resolution analysis of complex mixtures. *J. Magn. Reson* 1998;131:131–138. [PubMed: 9533915]
35. Nilsson M, Gil AM, Delgado I, Morris GA. Improving pulse sequences for 3D DOSY: COSY-IDOSY. *Chem. Comm* 2005:1737–1739. [PubMed: 15791316]
36. Nilsson M, Gil AM, Delgado I, Morris GA. Improving pulse sequences for 3D diffusion-ordered NMR spectroscopy: 2DJ-IDOSY. *Anal. Chem* 2004;76:5418–5422. [PubMed: 15362901]
37. These DOSY experiments are fairly fast and easy to be carried out. For example, it will usually take 10 minutes for  $^1\text{H}$  DOSY and 45 minutes for  $^{13}\text{C}$  INEPT DOSY to get a satisfactory spectrum for a 0.1M solution.



**FIGURE 1.**

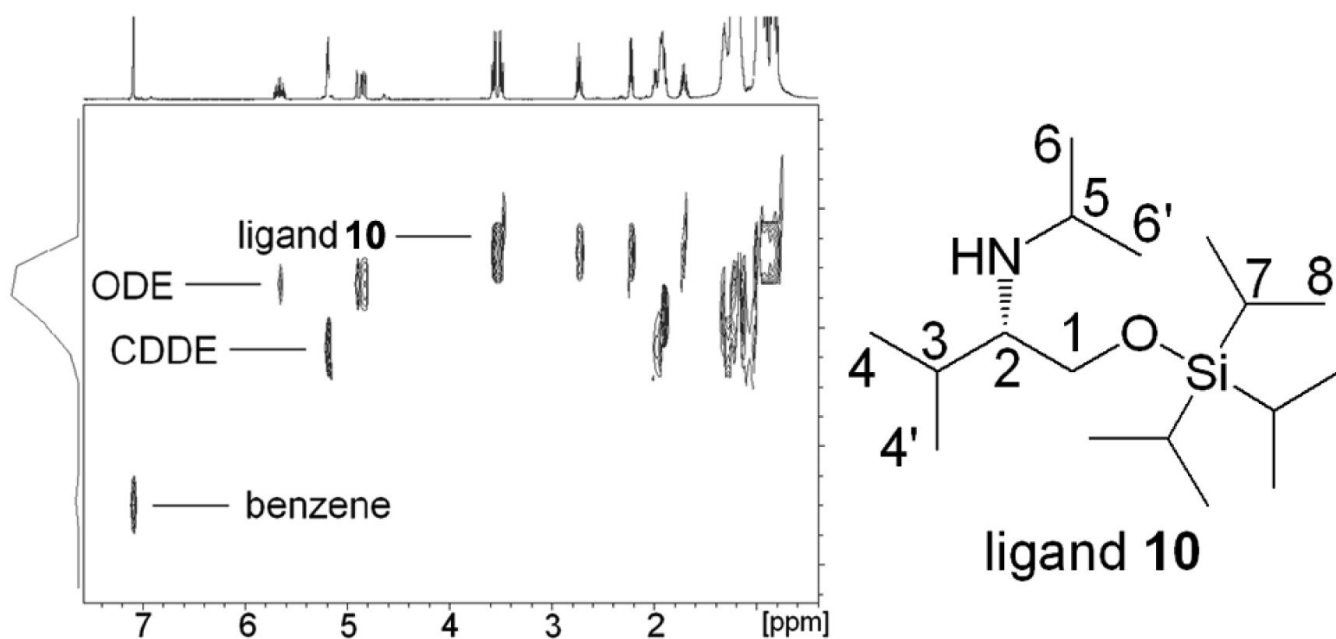
$^1\text{H}$  DOSY spectrum of *n*-BuLi in  $\text{THF-}d_8$  at  $-84\text{ }^\circ\text{C}$ . (a)  $^1\text{H}$  spectrum at 187 K, the labeled butyl resonances of dimeric (D) and tetrameric (T) *n*-BuLi were assigned by 2D-TOCSY. (b) 1D Slice of the DOSY spectrum at the diffusion coefficient of the tetramer (- - -). (c) 1D Slice of the DOSY spectrum at the diffusion coefficient of the dimer (-).



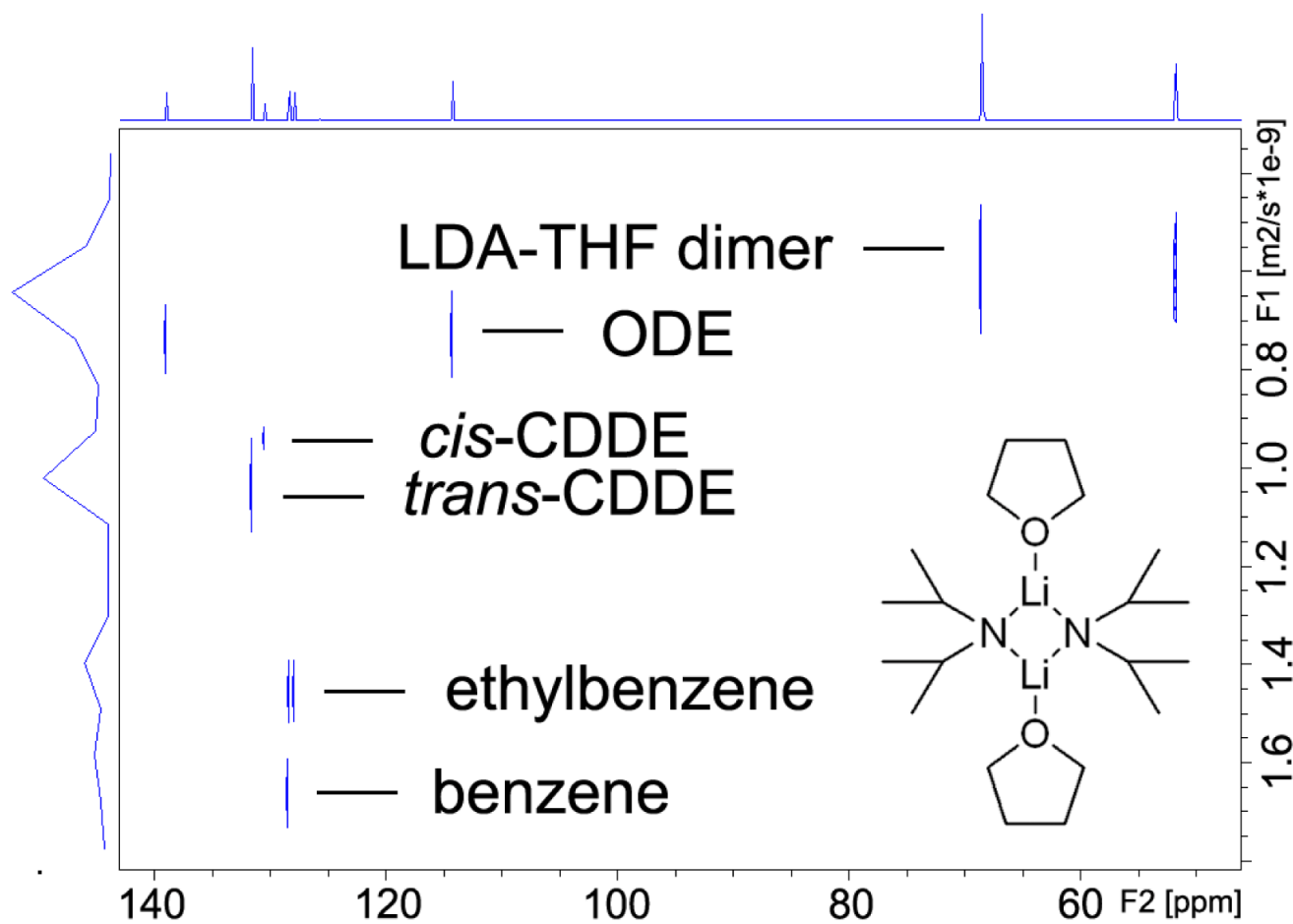
**FIGURE 2.**

<sup>1</sup>H PFG-DSTE NMR of *n*-BuLi in THF-*d*<sub>8</sub> at -84 °C. A typical Stejskal-Tanner plot of experimental peak areas: THF-*d*<sub>7</sub> (α-CDH), ■; THF-*d*<sub>7</sub> (β-CDH), □; tetramer (butyl α-CH<sub>2</sub> -1.00 ppm), •; and dimer (butyl α-CH<sub>2</sub> -1.12 ppm), ○. The solid lines represent linear least squares fits to the data.

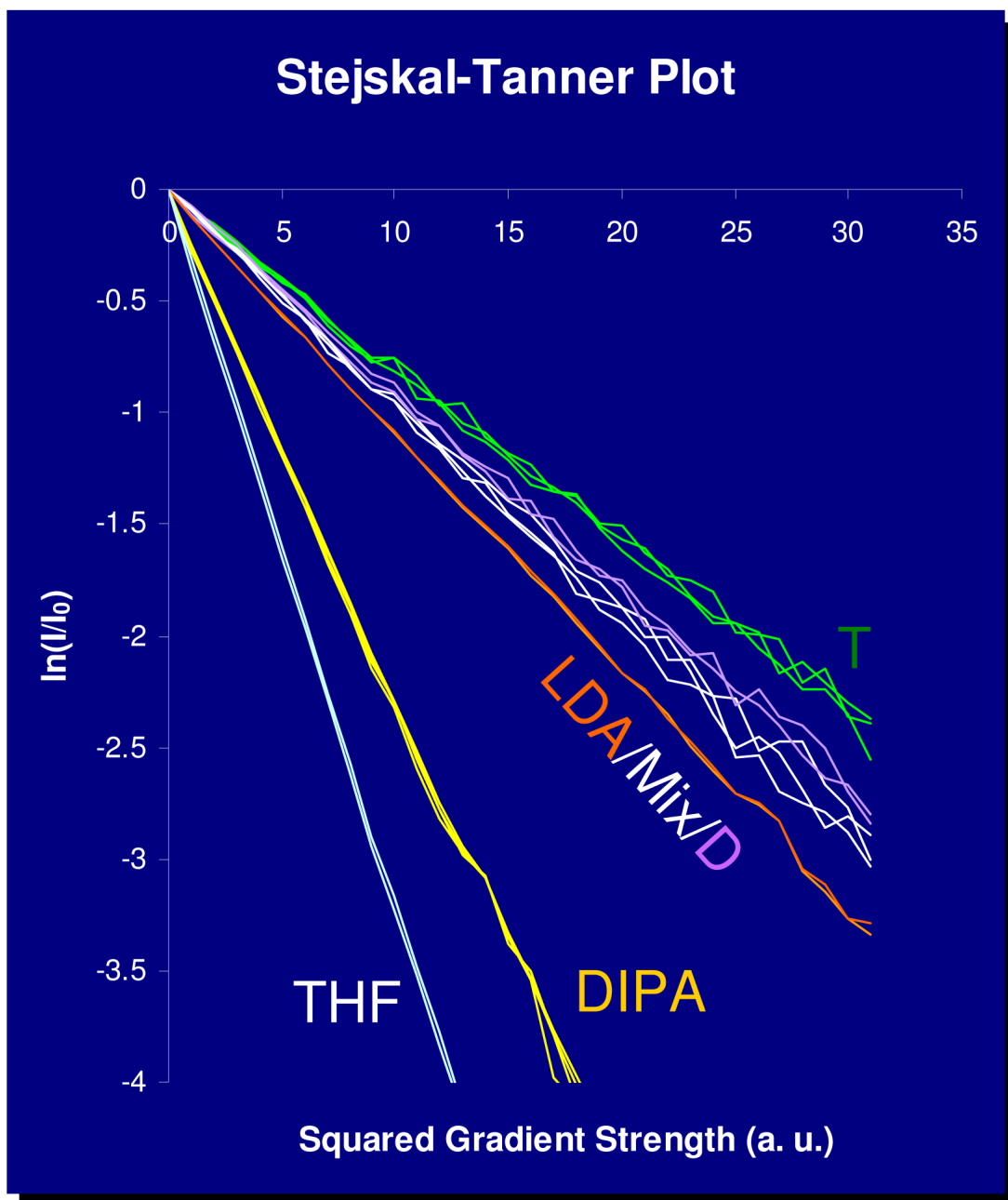




**FIGURE 3.** <sup>1</sup>H DOSY spectrum of ligand **10**, ODE, CDDE, and benzene in toluene-d<sub>8</sub>. X-axis represents the regular <sup>1</sup>H chemical shift and y-axis represents the relative diffusion rate.

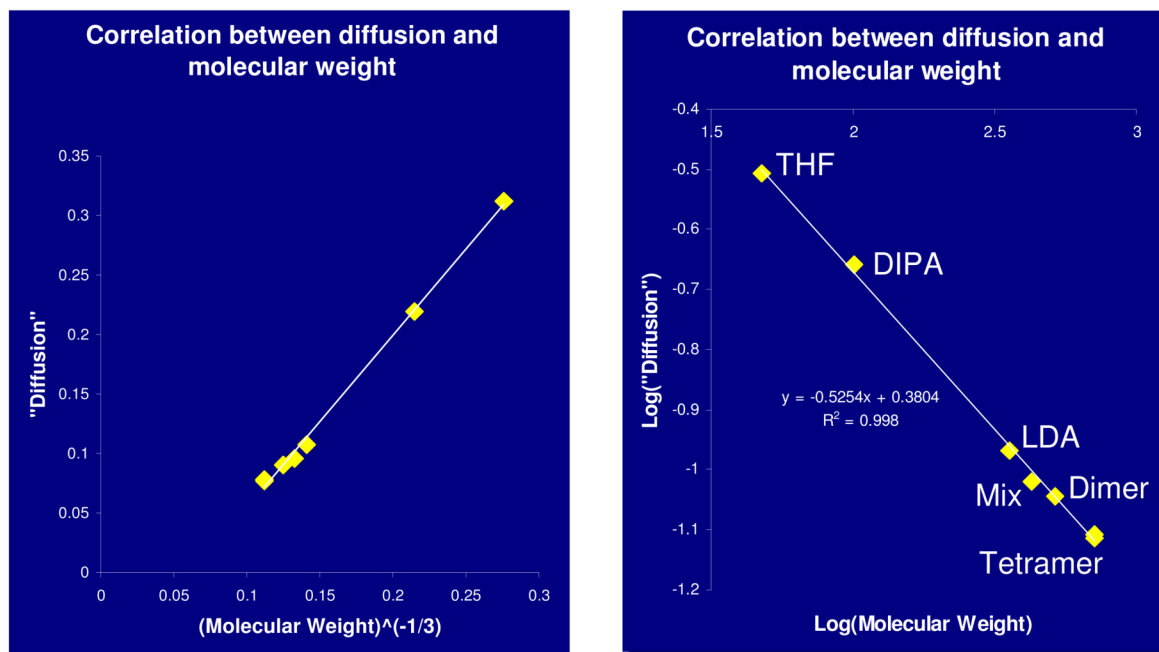
**FIGURE 4.**

$^{13}\text{C}$  INEPT DOSY of THF solvated LDA dimeric aggregate **6** in toluene- $d_8$  with internal references at 25 °C. The X-axis is the regular  $^{13}\text{C}$  INEPT dimension and the Y-axis is the diffusion dimension.



**FIGURE 5.**

$^1\text{H}$  PFG-DSTE DOSY NMR of LDA/LPN/DIPA/in THF- $d_8$  at  $-84^\circ\text{C}$ . Stejskal-Tanner plot of experimental peaks. Multiple peak areas are shown for each aggregate. (LDA: LDA dimer **6**; Mix: LPN/LDA mixed dimer **13**; D: LPN dimer **14**; T: LPN tetramer **15**.)

**FIGURE 6.**

$^1\text{H}$  PFG-DSTE DOSY NMR of LDA/LPN/DIPA/in THF- $d_8$  at  $-84$  °C. Plot of mobility as a function of  $\text{FW}^A$  ( $A = -1/3$ ) (left). Log-log plot of mobility as a function of FW (right). (LDA: LDA dimer **6**; Mix: LPN/LDA mixed dimer **13**; Dimer: LPN dimer **14**; Tetramer: LPN tetramer **15**.)

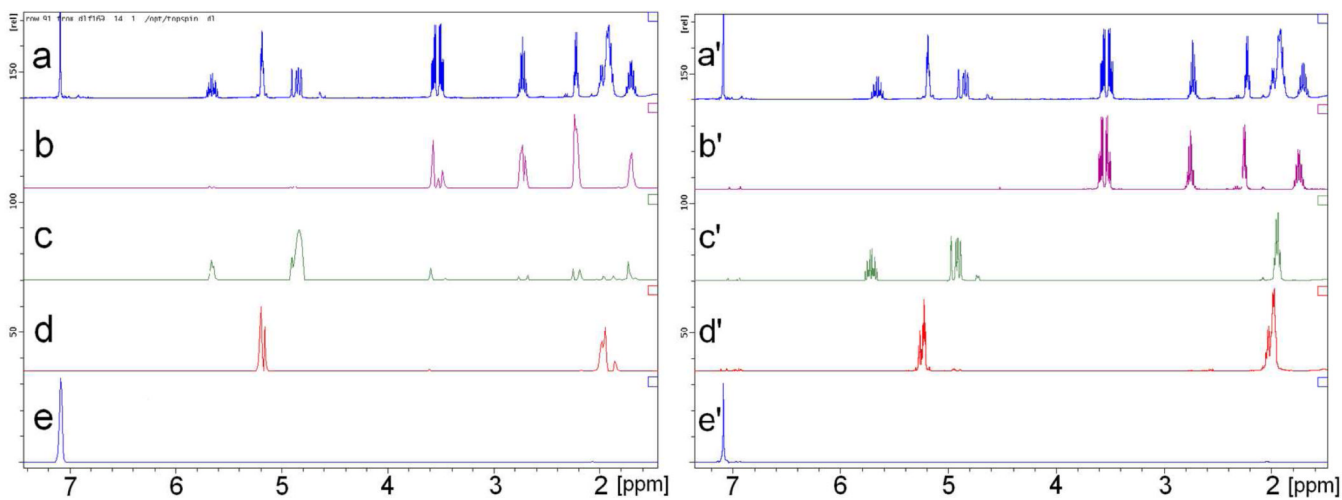


**FIGURE 7.**

Comparison between slices of  $^1\text{H}$  DOSY spectra (left) with  $^1\text{H}$  NMR spectra (right) of authentic samples. From top to bottom, slice or spectrum of ligand **10** with internal references (a/a'), ligand **10** without internal references (b/b'), ODE **21** (c/c'), CDDE **18** & **19** (d/d') and benzene **16** (e/e').



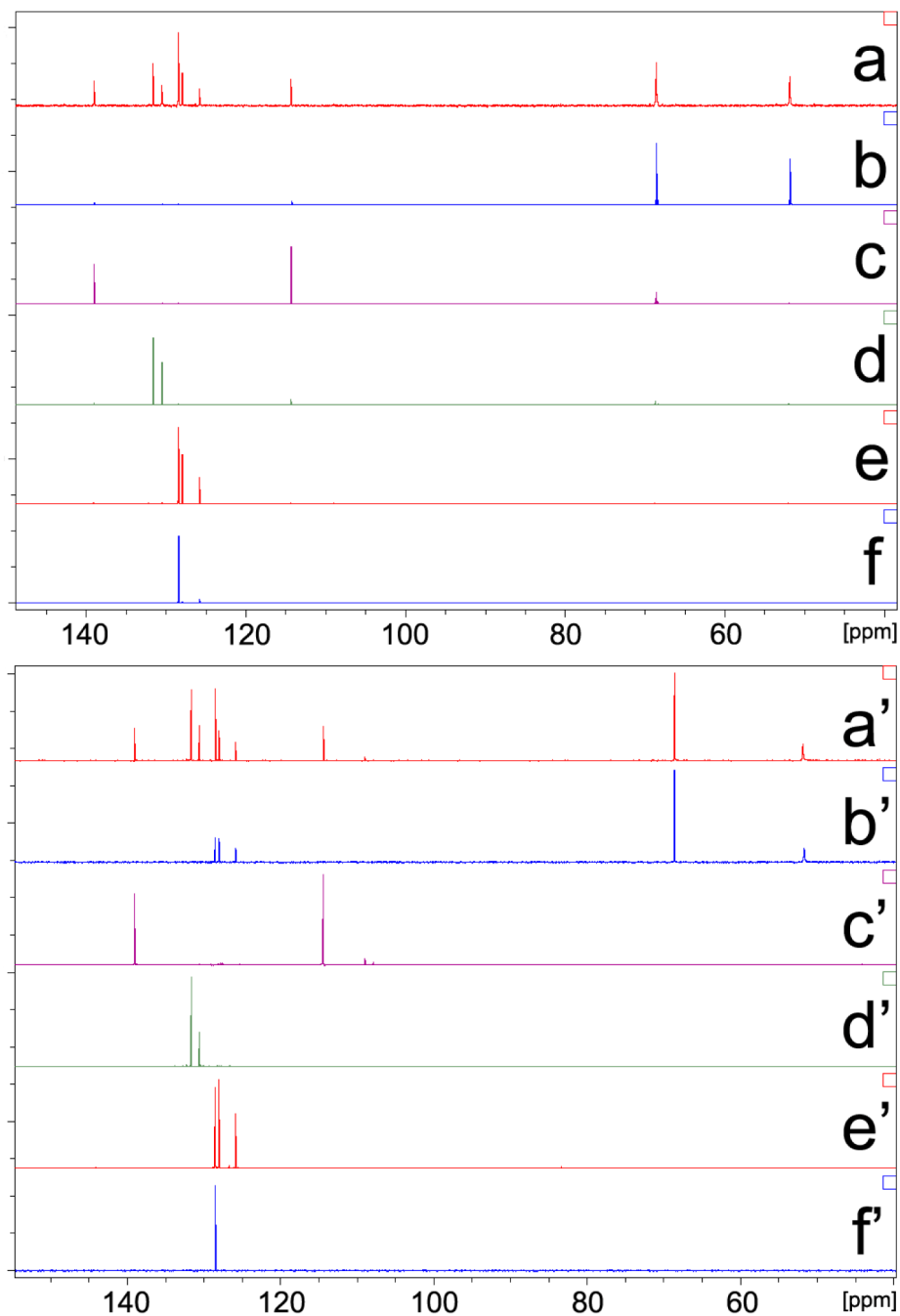


**FIGURE 8.** Comparison between slices of  $^{13}\text{C}$  INEPT DOSY spectra (a-f) with  $^{13}\text{C}$  INEPT NMR spectra of authentic samples (a'-f'). (a) and (a')-LDA dimer with internal references, (b) and (b')-LDA dimer without internal references, (c) and (c')-ODE, (d) and (d')-*cis*- and *trans*-CDDE mixture, (e) and (e')-ethylbenzene, (f) and (f')-benzene.

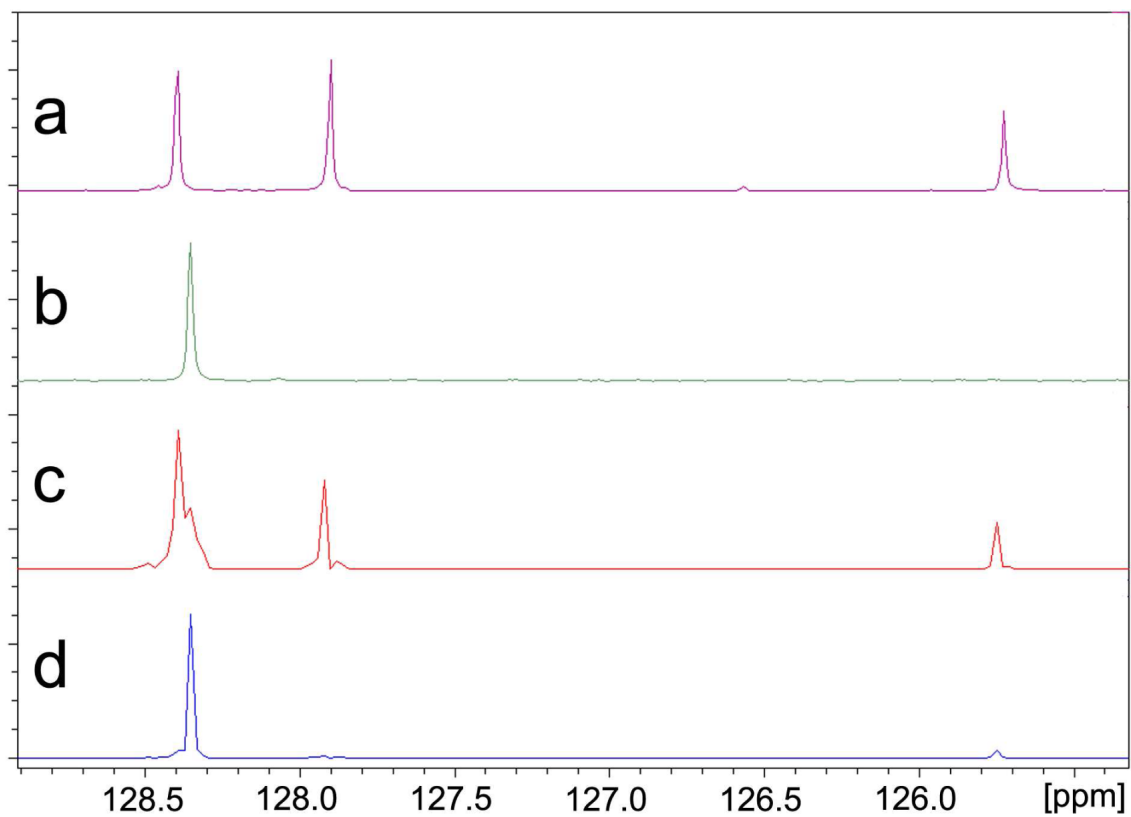


**FIGURE 9.** Comparison of the  $^{13}\text{C}$  INEPT spectra of ethylbenzene and benzene to the  $^{13}\text{C}$  INEPT DOSY slices of ethylbenzene and benzene. (a)  $^{13}\text{C}$  INEPT of ethylbenzene, (b)  $^{13}\text{C}$  INEPT of benzene, (c) DOSY slice of ethylbenzene, (d) DOSY slice of benzene.

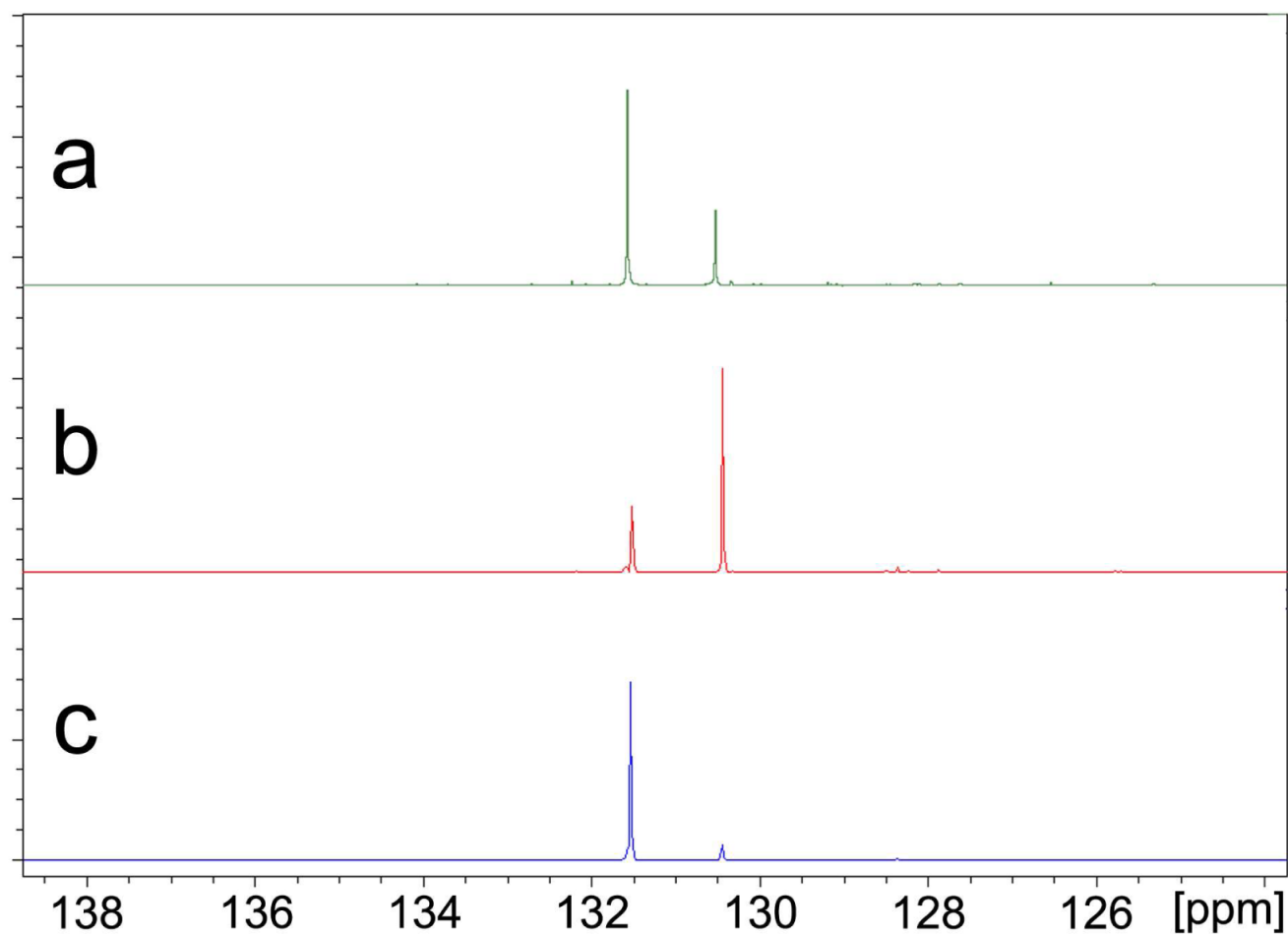


**FIGURE 10.** Comparison of the  $^{13}\text{C}$  INEPT spectrum of *cis*- and *trans*-CDDE mixture to the  $^{13}\text{C}$  INEPT DOSY slices of *cis*-CDDE and *trans*-CDDE. (a)  $^{13}\text{C}$  INEPT of *cis*- and *trans*-CDDE mixture, (b) DOSY slice of *cis*-CDDE, (c) DOSY slice of *trans*-CDDE.

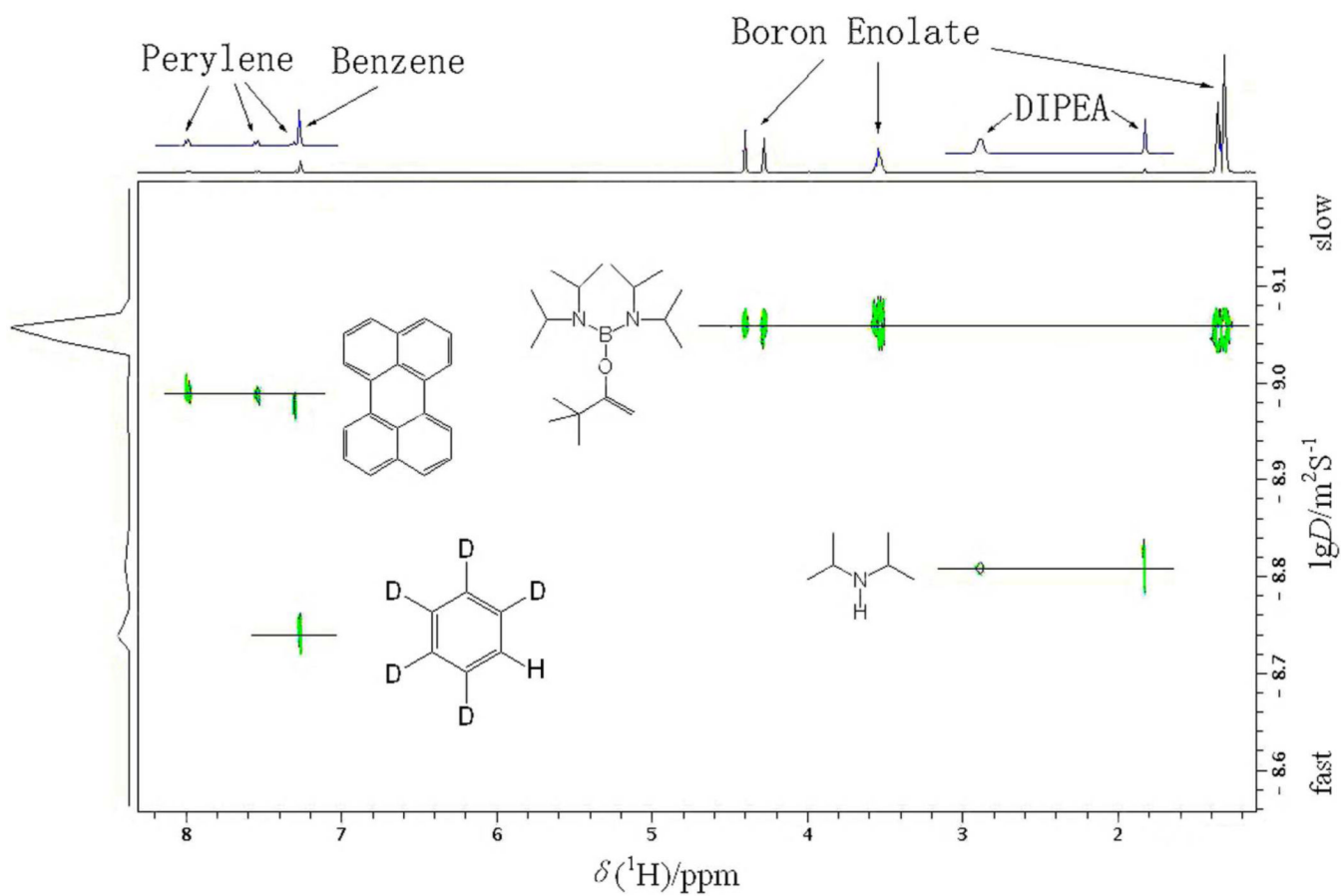


**FIGURE 11.**  $^1\text{H}$  DOSY NMR ( $\text{C}_6\text{D}_6$ , 400 MHz) of boron enolate **5**, perylene **17**, DIPEA **12**, and benzene- $\text{d}_6$ .

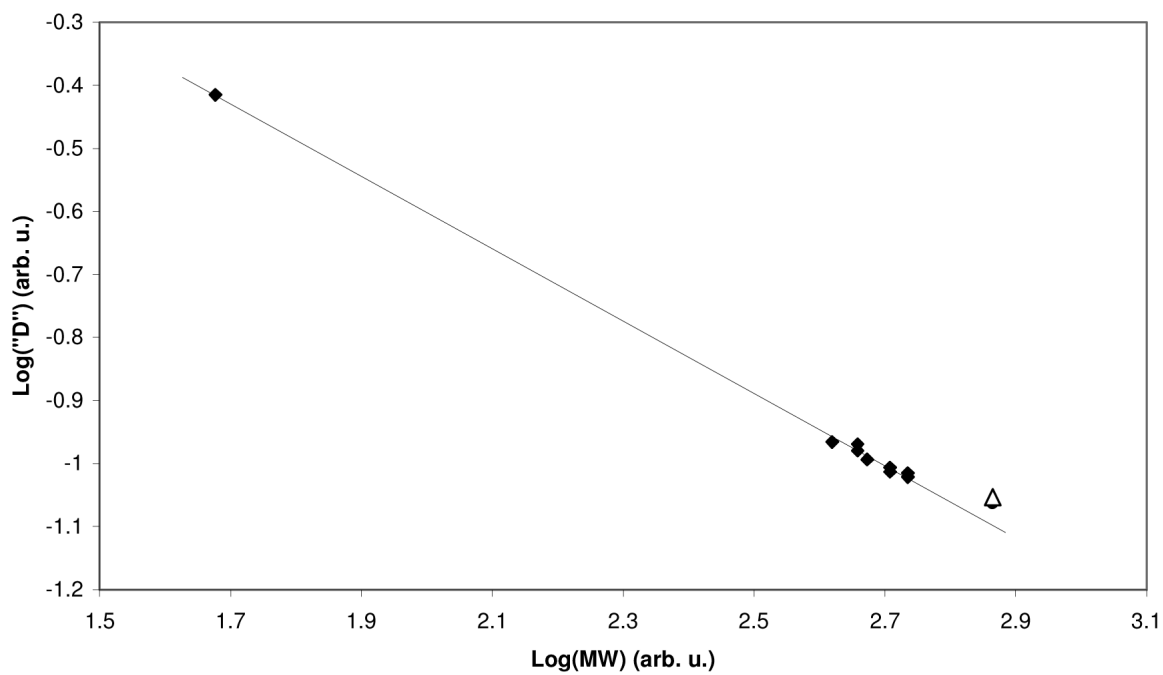


**FIGURE 12.**

DOSY of the major aggregates (**26-30**) at  $-80\text{ }^{\circ}\text{C}$ . The solid line is linear least squares fit to the data points represented by diamonds. The triangle represents the tetramer **28**, and was not included in the fit.



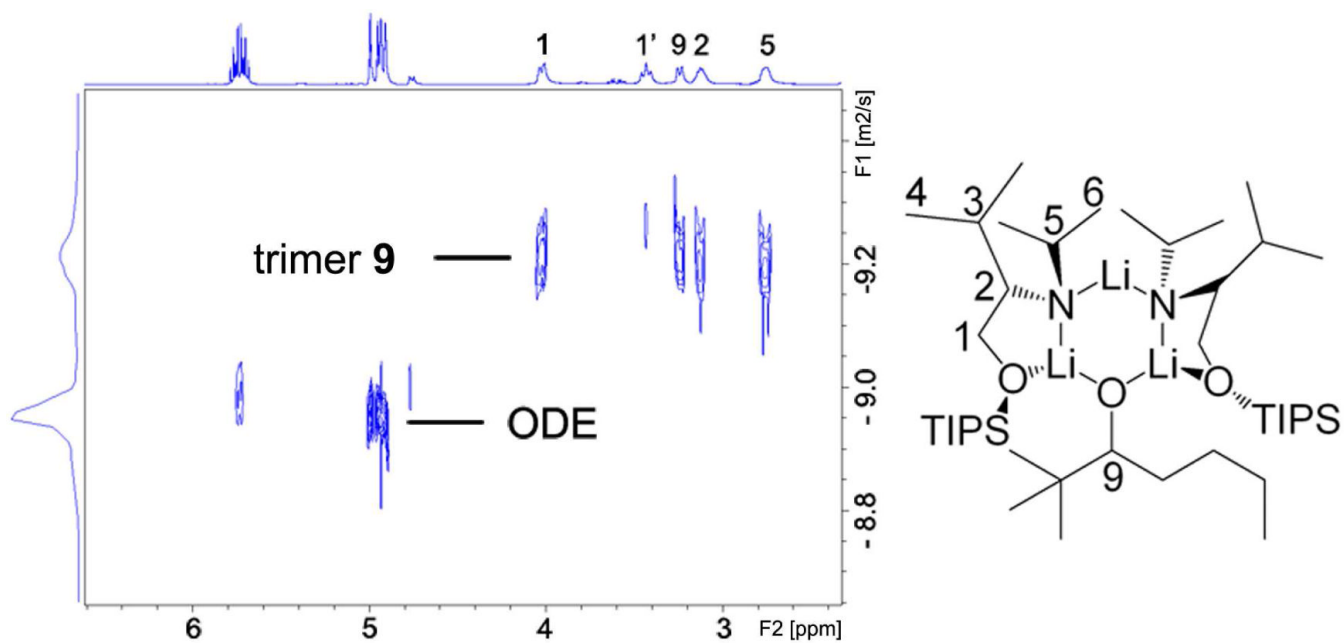


**FIGURE 13.**  
 $^1\text{H}$  DOSY of trimeric complex **9** and ODE in toluene- $d_8$  at 25  $^\circ\text{C}$ .

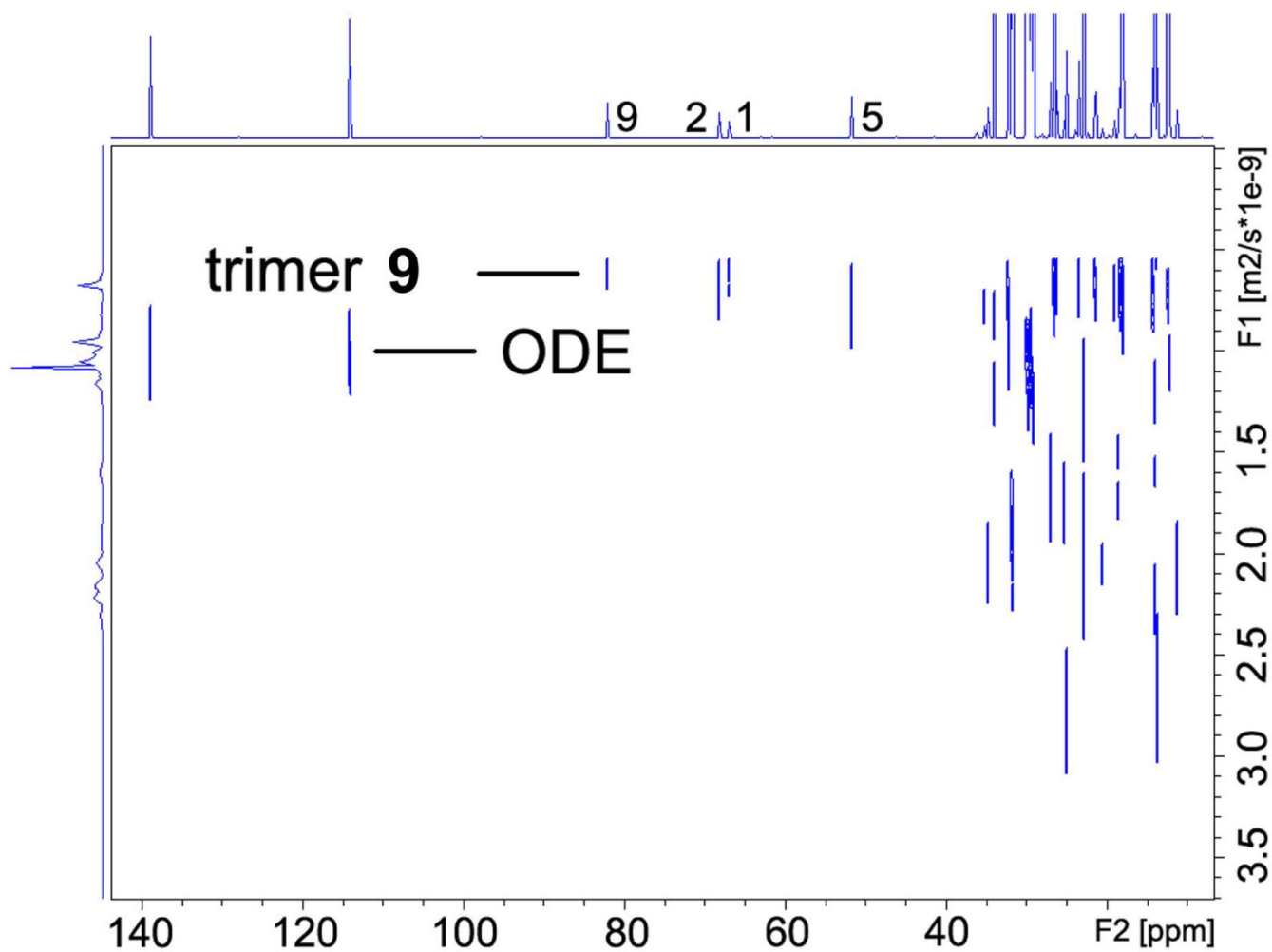
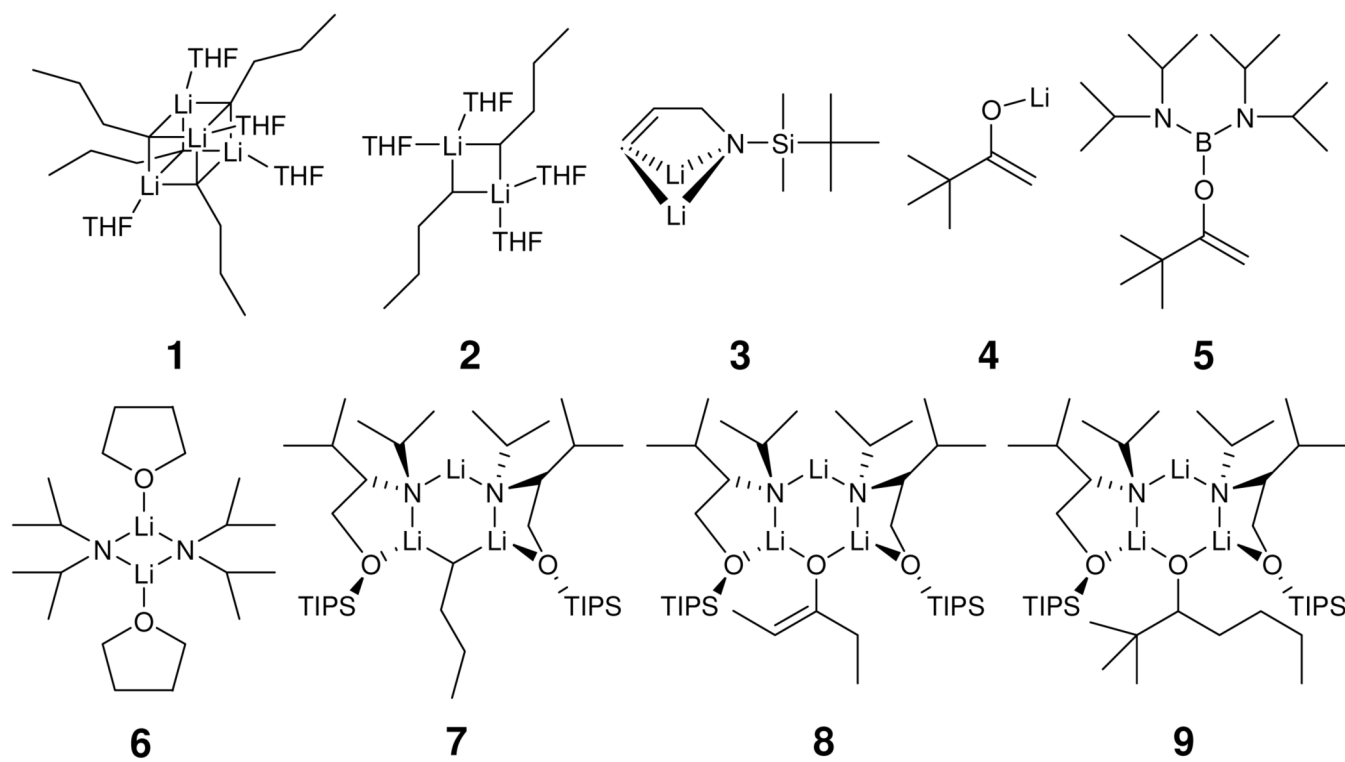
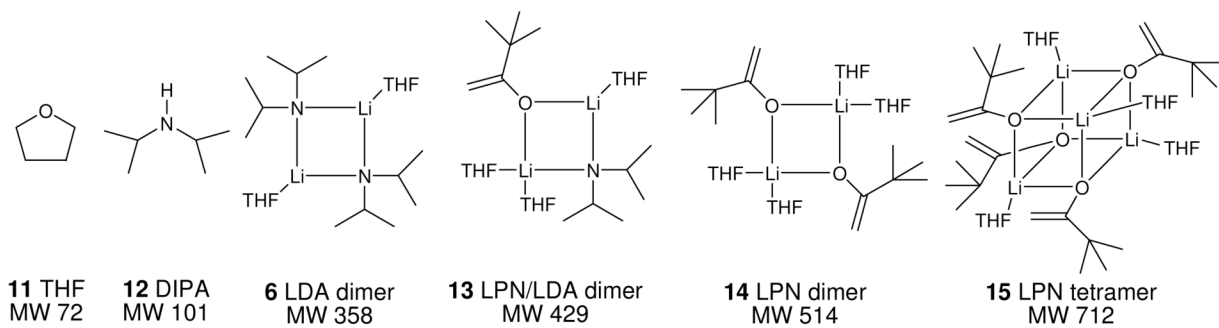


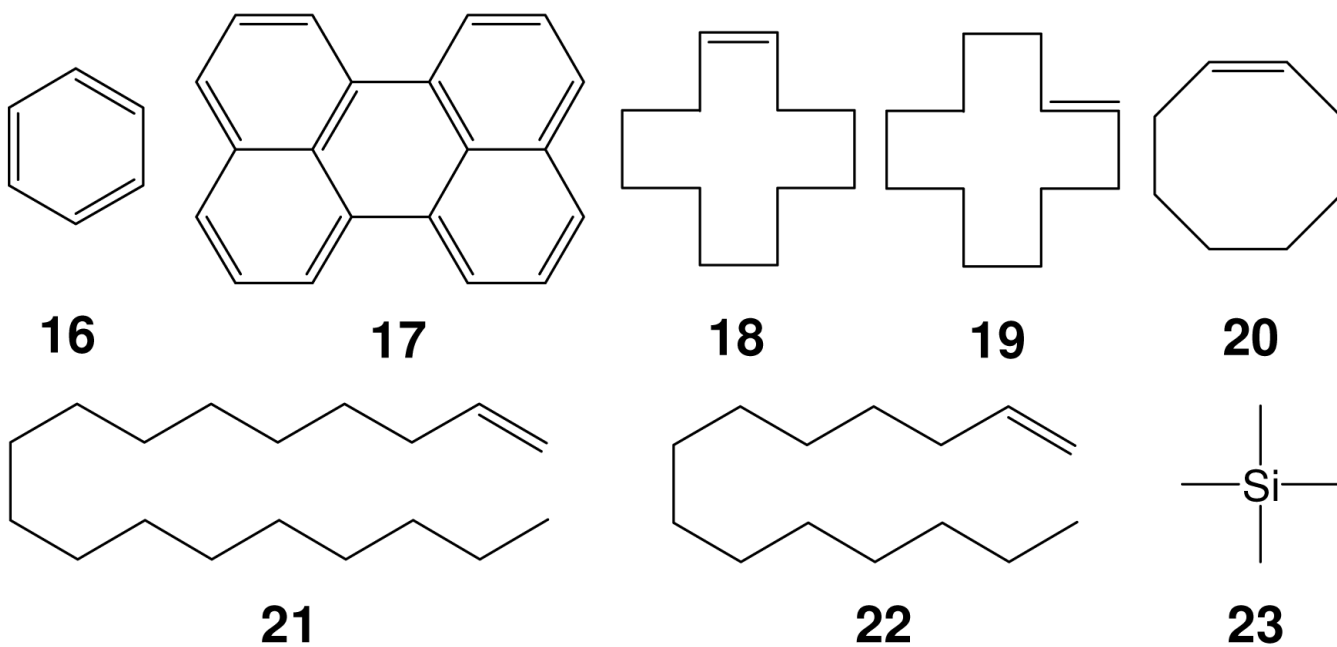
**FIGURE 14.**  
 $^{13}\text{C}$  INEPT DOSY of complex **9** and ODE in toluene- $d_8$  at 25 °C.



**SCHEME 1.**  
Reactive intermediates investigated in our lab.

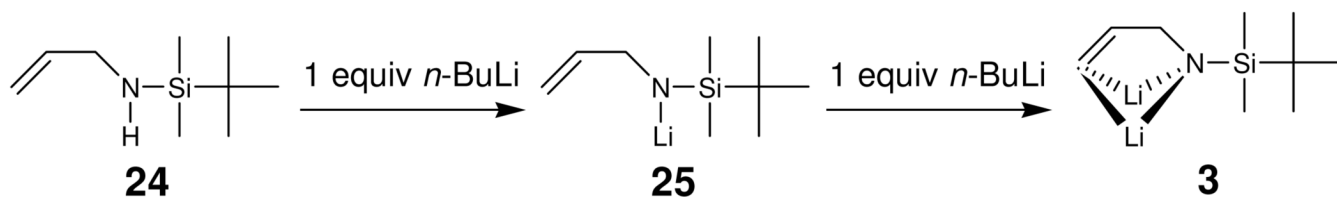


**SCHEME 2.**  
LDA and LPN aggregates in THF.

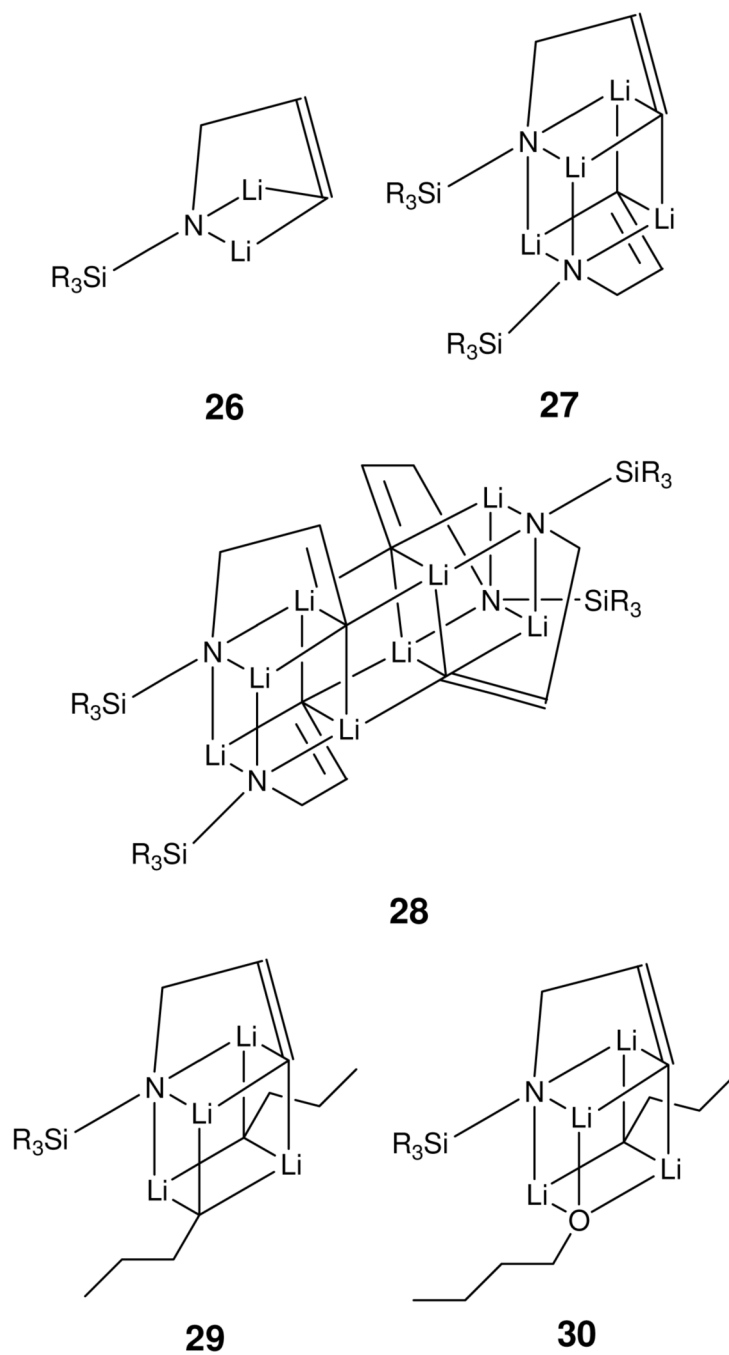


**SCHEME 3.**  
Four type internal references.

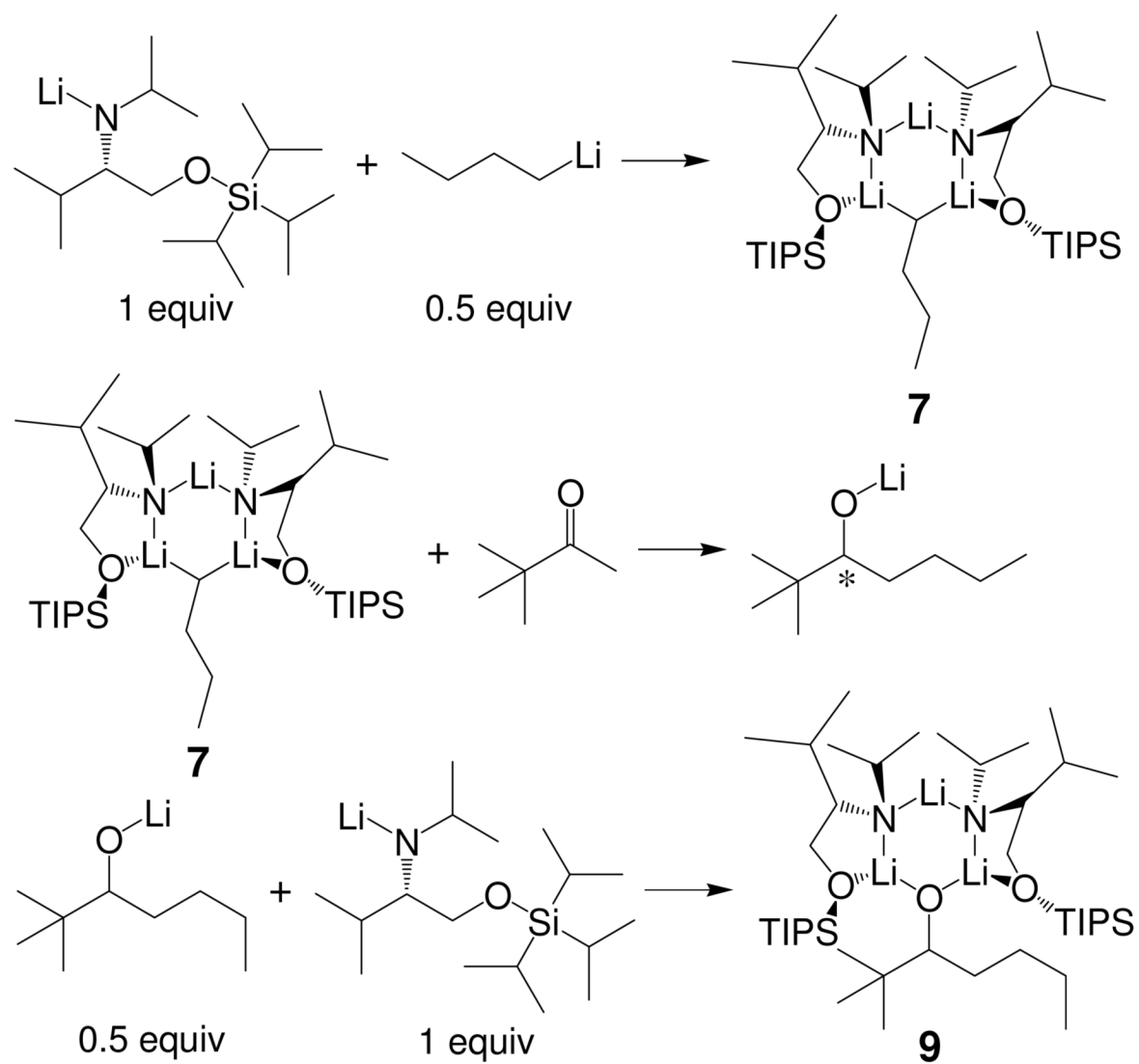




SCHEME 4.



**SCHEME 5.**  
Aggregates of intermediate **3**. ( $\text{SiR}_3 = \text{TBDMS}$ )



SCHEME 6.

TABLE 1

DOSY of the aggregates in THF-d<sub>8</sub> at -80 °C.

	26	27	28	29	30	1
<b>3</b>	1	2	4	1	1	0
<i>n</i> -BuLi	0	0	0	2	1	2
<i>n</i> -BuLi	0	0	0	0	1	0
THF	5	2	0	2	2	4
FW	543	510	732	455	471	416